論文の内容の要旨

論文題目

Anion photoelectron spectroscopy and ion mobility mass spectrometry on chemically-synthesized gold clusters in gas phase

(化学的に合成された金クラスターの
気相中における負イオン光電子分光とイオン移動度質量分析)

氏名：平田圭祐

1. Introduction

Ligand (L)-protected gold clusters with atomically-defined sizes, $[Au_xL_y]^z$, provide us with an ideal platform to study size-dependent evolution of structures and properties of gold in nanoscale. Geometric and electronic structures of these chemically-synthesized Au clusters have been revealed by single-crystal X-ray diffraction (SCXRD), X-ray and UV-vis absorption spectroscopy, cyclic voltammetry and so on. However, experimental methods in the gas phase further give us valuable information on intrinsic physical properties and elemental excitation and relaxation processes without perturbation from the surrounding environment. For example, ion mobility mass spectrometry (IMMS) allows us to determine collision cross section (CCS) and to monitor collision-induced structural isomerization processes of $[Au_xL_y]^z$ in the electronically ground state (Figure 1). Photoelectron spectroscopy (PES) and photodissociation mass spectrometry (PDMS) determine the electron affinity and probe photo-induced relaxation processes including dissociation and delayed electron emission (Figure 1). In my thesis, I conducted PES and PDMS on $[Au_{25}(SR)_{18}]^-$ (RS = thiolate) to determine the electron affinity and to probe relaxation processes upon photoexcitation. I also conducted IMMS on $[PdAu_8(PPh_3)_8]^{2+}$

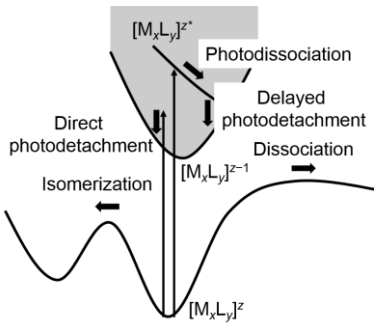

Figure 1. Schematic illustration of excitation and relaxation processes of $[Au_xL_y]^z$.

and $[Au_9(PPh_3)_8]^{3+}$ to reveal whether the structures of the cluster in the gas phase are same with those determined by SCXRD and whether the isomerization can be induced upon collisional excitation.

2. Photoelectron detachment and photo-induced thermionic emission: $[Au_{25}(SR)_{18}]^-$

Anion PES and PDMS were conducted on a representative thiolate-protected Au cluster, $[Au_{25}(SR)_{18}]^-$, having an icosahedral Au_{13} core protected by six $Au_2(SR)_3$ oligomers and a quantized electronic structure with a closed superatomic electron configuration of $(1S)^2(1P)^6$ [1,2]. Single crystal structure and optical absorption spectrum of $[Au_{25}(PET)_{18}]^-$ (PET = phenylethanethiol) are shown in Figure 2 [1]. The experimental apparatus used consists of an ESI source, a TOFMS, and a magnetic-bottle photoelectron spectrometer as shown in Figure 3. PD mass spectra and PE spectra were recorded by detecting fragment ions and electrons, respectively, generated upon irradiation of a third/fourth harmonic output of a Nd:YAG laser (355/266 nm) onto mass-selected beam of $[Au_{25}(SR)_{18}]^-$ introduced into vacuum via the ESI source.

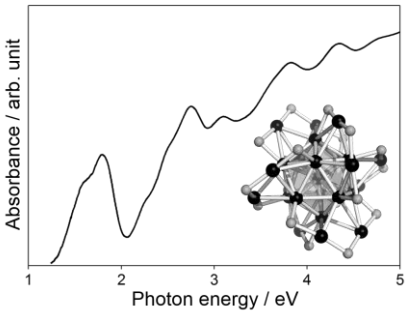

Figure 2. Absorption spectrum of $[Au_{25}(PET)_{18}]^-$. Inset shows the crystal structure of $[Au_{25}(PET)_{18}]^-$. C and H atoms are omitted for clarity.

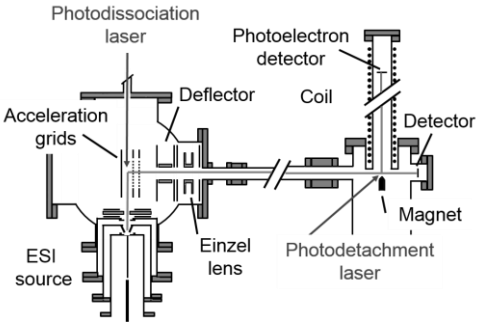

Figure. 3. Experimental apparatus for anion PES and PD MS.

The PE spectrum of $[Au_{25}(SC_{12}H_{25})_{18}]^-$ recorded at 355 nm exhibited two bands A and B (Figure 4a), which are assigned to the direct electron detachment from a 1P superatomic orbital and from 5d orbital localized on Au atoms, respectively. The adiabatic electron affinity (AEA) of $[Au_{25}(SC_{12}H_{25})_{18}]^0$ and vertical detachment energy (VDE) of $[Au_{25}(SC_{12}H_{25})_{18}]^-$ were determined for the first time to be 2.2 and 2.5 eV from the onset (E_{th}) and the top (E_{top}) of band A, respectively. The PD mass spectrum recorded at 355 nm revealed that photodissociation into $[Au_{21}(SC_{12}H_{25})_{14}]^-$ and $Au_4(SC_{12}H_{25})_4$ proceeded as a minor process with a branching fraction of <5%.

Interestingly, the PE spectrum of $[Au_{25}(PET)_{18}]^-$ recorded at 266 nm (Figure 4b) exhibited a

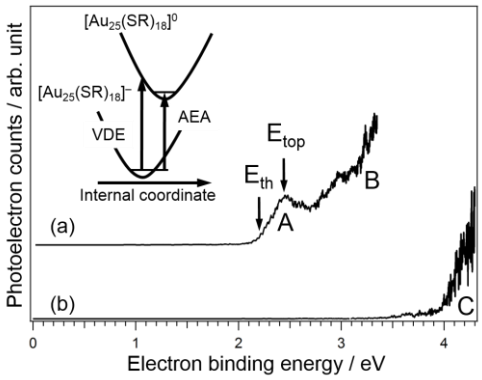

Figure. 4. Photoelectron spectra of (a) $[Au_{25}(SC_{12}H_{25})_{18}]^-$ at 355 nm and (b) $[Au_{25}(PET)_{18}]^-$ at 266 nm. Inset shows schematic potential energy curves of $[Au_{25}(SR)_{18}]^-$ and $[Au_{25}(SR)_{18}]^0$.

completely different profile from that at 355 nm. The PE spectrum was dominated by an intense band C at >4.0 eV, indicating slow (kinetic energy <0.7 eV) electron emission is dominant over direct electron detachment. Band C was assigned to thermionic emission (TE) from vibrationally excited $[Au_{25}(PET)_{18}]^-$ because of the exponential-like profile [3]. The PD mass spectrum of $[Au_{25}(PET)_{18}]^-$ at 266 nm did not show any fragment ions. These observations at 266 nm can be explained in such a manner that $[Au_{25}(PET)_{18}]^-$ is excited selectively to an electronically excited state (Figure 2) embedded in the electron detachment continuum, quickly relaxed to the ground state by dissipating the absorbed energy into internal degrees of freedom, and emit a slow electron from the cluster thus heated. The TE process observed is in sharp contrast to the direct photoelectron detachment from bare Au cluster anions and is ascribed to the suppression of the fragmentation pathways by the protection with the stiff $Au_2(SR)_3$ oligomers [4].

3. Collision-induced isomerization: $[PdAu_8(PPh_3)_8]^{2+}$ and $[Au_9(PPh_3)_8]^{3+}$

$[PdAu_8(PPh_3)_8]^{2+}$ and $[Au_9(PPh_3)_8]^{3+}$ were synthesized according to the methods reported [5]. In the following, I focused on the result on $[PdAu_8(PPh_3)_8]^{2+}$, whose crystal structure is shown in Figure 5 [6]. Figure 6 shows a schematic diagram of the IMMS apparatus installed at Indian Institute of Technology, Madras. The $[PdAu_8(PPh_3)_8]^{2+}$ clusters dispersed in methanol were introduced into the quadrupole mass filter via the electrospray ionization (ESI) source. The mass-selected cationic clusters were periodically injected into the He cell and traveling wave ion mobility (TWIM) cell. Gas pressures in the He and TWIM cells were controlled by the flow rates of He (F_{He}) and N_2 in the range of 0–150 and 45–55 mL min^{-1}, respectively. The ions in the TWIM cell were propelled by a continuous sequence of an electric field traveling through the cell and lost a part of the energy in collision with He gas. Ions with a small CCS are ejected from the TWIM cell earlier than those with a high CCS. The ions thus separated based on CCS were detected by a time-of-flight mass spectrometer (TOFMS). Arrival time distribution (ATD) was obtained by plotting the intensity of $[PdAu_8(PPh_3)_8]^{2+}$ as a function of the time difference, T_{AT}, between the ion injection and ion extraction at the TOFMS.

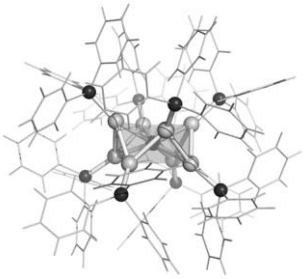

Figure 5. Crystal structure of $[PdAu_8(PPh_3)_8]^{2+}$. Ph groups are shown by wireframe.

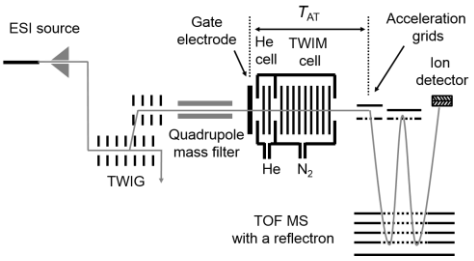

Figure 6. Schematic diagram of the IM MS apparatus.

Figure 7 shows typical ATDs of $[PdAu_8(PPh_3)_8]^{2+}$ as a function of F_{He}. The ATD at F_{He} = 150 mL min^{-1} exhibits a single peak β. When F_{He} is reduced to 80 mL min^{-1}, a new peak α emerges as a hump at the shorter arrival time side of peak β and becomes dominant with decrease in F_{He}.

With the decrease in F_{He}, the ions in the He cell gain more kinetic energy from the traveling electric field due to the decrease in collision frequency and, as a result, collide with N_2 with a higher collision energy. Therefore, the transformation from peak β to α indicates that the isomer for peak β ($PdAu_8$(B)) is converted to a more compact isomer for peak α ($PdAu_8$(A)) by collisional heating. The CCS values for $PdAu_8$(A) and $PdAu_8$(B) were experimentally determined to be 404 and 422 Å^2, respectively. In the crystal, the PPh_3 layer of $[PdAu_8(PPh_3)_8]^{2+}$ constructs a densely packed structure due to CH–π interactions between the phenyl groups of adjacent PPh_3 ligands. Because no other isomer having a more compact packing than the crystal structure is available, $PdAu_8$(A) is assigned to the densely packed ligand layer similar to that in crystal.

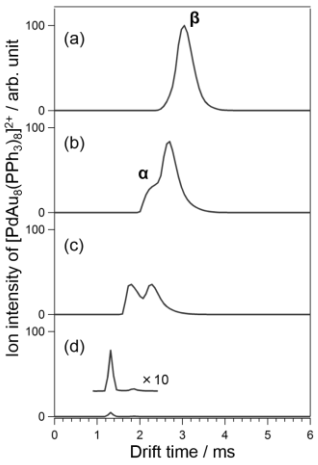

Figure 7. ATDs of $[PdAu_8(PPh_3)_8]^{2+}$ at F_{He} = (a) 150, (b) 80, (c) 43, and (d) 0 mL min^{-1}.

Since no other isomer with a different core motif is known, it is reasonable to assign $PdAu_8$(B) to an isomer having poorly packed ligand structures. Similar results were obtained for $[Au_9(PPh_3)_8]^{3+}$. It is concluded from these results that disordered ligand layers of $[PdAu_8(PPh_3)_8]^{2+}$ and $[Au_9(PPh_3)_8]^{3+}$ in dispersing media are frozen during the ESI process and that they are annealed to the most stable, densely packed structure similar to those in the crystals upon the vibrational excitation by collision with He gas.

4. Conclusion

The PE spectrum at 355 nm exhibited two bands that were assigned to the electron detachment from a 1P superatomic orbital and from 5d orbital localized on Au atoms. The AEA of $[Au_{25}(SC_{12}H_{25})_{18}]^0$ and VDE of $[Au_{25}(SC_{12}H_{25})_{18}]^-$ were determined to be 2.2 and 2.5 eV, respectively. The TE process observed at 266 nm is ascribed to selective excitation into an electronically excited state in the electron detachment continuum and the suppression of the fragmentation by the protection of the surface Au atoms with the stiff $Au_2(SR)_3$ oligomers. IM MS study revealed that less packed ligand layers of $[PdAu_8(PPh_3)_8]^{2+}$ and $[Au_9(PPh_3)_8]^{3+}$ were converted to densely packed ones by collisional activation and cooling.

Acknowledgments

I thank Prof. T. Pradeep (IIT Madras) for giving me an opportunity to use an ion mobility mass spectrometer and Dr. Takashi Nagata (SOKENDAI) for providing us with their PES machine.

References

[1] Zhu, M. *et al*., *J. Am. Chem. Soc*. **2008**, *130*, 5883. [2] Walter, M. *et al*., *Proc. Natl Acad. Sci. USA* **2008**, *105*, 9157. [3] Weidele, H. *et al*., *Chem. Phys. Lett.* **1995**, *237*, 425. [4] Yamazoe, S. *et al*., *Nature Chem*. **2016**, *7*, 10414. [5] Yamazoe, S. *et al*., *Inorg. Chem*. **2017**, *56*, 8319. [6] Matsuo, S. *et al*., *ChemElectroChem* **2016**, *3*, 1206.